



Chemical preparation and physicochemical characterization of powdered activated carbons based on safou (*Dacryodes edulis*) seeds

C.D. Atemkeng¹, T. Kamgaing¹, D.R. Tchuifon Tchuifon^{1,2},
G. Doungmo³, L.A. Amola¹, A.T. Kamdem⁴, S.G. Anagho^{1,5*}

¹Research Unit of Noxious Chemistry and Environmental Engineering, Department of Chemistry, Faculty of Science, University of Dschang P.O. Box 67, Dschang, Cameroon,

²Department of Chemical and Process Engineering, National Higher Polytechnic School of Douala, University of Douala, P.O. Box 2701 Douala, Cameroon

³Institute of Inorganic Chemistry, Christian-Albrechts-Universität zu Kiel, Max-Eyth-Str. 2, 24118 Kiel, Germany,

⁴Laboratory for sensors, Institute of Microsystems Engineering-IMTEK, University of Freiburg, Georges-Koelher -Allee 103, 79110 Freiburg, Germany Freiburg Materials Research Center - University of Freiburg, Stefan Meier Strasse 21, 79104 Freiburg, Germany,

⁵Department of Chemistry, Faculty of Science, University of Bamenda, P.O. Box 39 Bamili, Cameroon

Received 16 March 2020,
Revised 20 May 2020,
Accepted 21 May 2020

Keywords

- ✓ safou seed
- ✓ activated carbon
- ✓ optimization
- ✓ physicochemical characterization.
- ✓ response surface methodology

Solomon GABCHE ANAGHO
sg_anagho@yahoo.com ;
Phone: +237 677 578 567;

Abstract

Two activated carbons (ACs) obtained from safou seeds, an abundant agricultural residue considered as waste, were chemically prepared using H_3PO_4 and H_2SO_4 as activating reagents, using an impregnation ratio of 60% relative to the mass of the precursor. The ACs obtained from H_3PO_4 and H_2SO_4 were labelled respectively as NSPT and NSST. The central composite design (CCD) with three centre points was adopted to optimize the operating conditions for producing the activated carbons. Three important parameters were considered: concentration of the activating agent, temperature and duration of calcination. The expected response was the iodine number. To better observe the correlation between the significant factors influencing this response, the analysis of variance (ANOVA) through t-test, response surface, Pareto diagram and influence of each of the factors taken individually were exploited. With regard to the NSPT activated carbon, the iodine number was 838.5 mg.g^{-1} and for the NSST activated carbon, it was 822.5 mg.g^{-1} . Under optimal conditions generated from STATGRAPHICS Plus version 5.0 software used in this work, the mass of the activated carbon yields were 53.41% and 38.85% respectively for NSPT and NSST. The functional surfaces of the two activated carbons were established by Boehm titration, pH, pH_{ZPC} and FT-IR techniques. Moreover, the activated carbons were submitted to some analysis such as TGA/TDA, DRX, and BET/BJ to have information about their structural and physicochemical properties.

1. Introduction

By-products generated from agricultural activities are quite abundant and they can be highly polluting to the environment when allowed to decay. That is, when they are abandoned in nature over a period of time, they biodegrade and become toxic to the environment [1]. Furthermore, they are not usually used as a food resource for animals [2]. Coconut shell, empty cocoa pods, sea shells, to name just a few are all agricultural residues that if valued, would considerably generate additional income to the agro based industries. Several techniques have been developed by researchers to minimize the presence of agricultural wastes in the environment and above all to give them a market value [3], [4], [5]. They are most often low-porous lignocellulosic materials whose carbonization can improve their adsorbent properties by processing them into activated carbons with high reactivity, provided they are abundant and available [6].

Numerous studies have been devoted to the production and characterization of activated carbons from various materials of plant origin such as rice straws [5], [7], [8], coconut shell [9], sugar beet bagasse [10], peanut shells [2], apricot shells [11], bitter kola nut shells [12], rice husks [13] and many others. The present study is focused on safou residues (*Dacryodes edulis*). The choice of this biomass was first motivated by its abundance; with an annual output of 13,000 tonnes/year [14] and by the work of Kamgaing *et al.* (2017) [15] in which they used these raw safou seeds to remove bisphenol A from solution with promising results. To our knowledge of the literature, safou seeds have not yet been exploited as a precursor for the production of activated carbons. Furthermore, it is well known from the literature that, the carbonization process in preparing activated carbons from starting biomass materials generally enhance their properties. The objective of this work was to chemically produce porous activated carbons from the safou seed residue with appreciable iodine number by using the response surface methodology to obtain the optimum preparation conditions

2. Materials and methods

2.1 Collection and pretreatment of the precursor material

Safou residues used in this work are agricultural residues that were collected from traders in the city of Dschang, Cameroon. They were thoroughly washed with running water, rinsed with distilled water and left in open air to dry off the water before drying in a Binder oven. The dried seeds were ground and sieved to obtain particles of sizes less than 2 millimeters. These particles of small size were calcined to obtain the activated carbon which was subsequently kept in a desiccator as presented in figure 1.

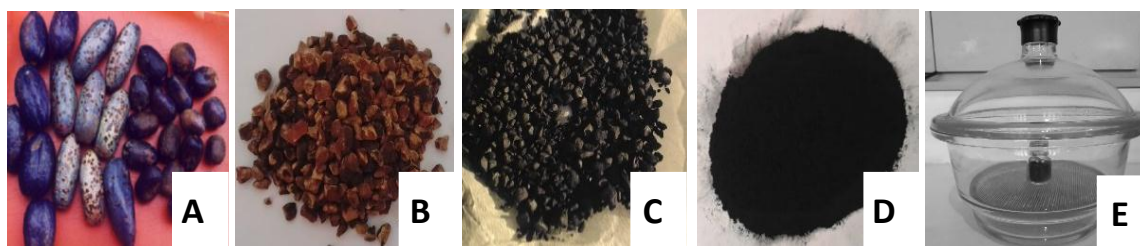


Figure 1 : Safou : fruit (A), seeds (B), granular activated carbon (C) powdery activated carbon (D) and conservation in a desiccator (E).

2.2 Chemical activation of the precursor material

The particles of desired diameters were impregnated respectively with phosphoric acid and sulfuric acid. The impregnation was done in a ratio of 60% relative to the mass of the precursor. Once the precursor was impregnated with the activating agent, the mixtures were stirred at 25°C for 24 hours, then filtered. The residue from the filtration were dried in an oven at a temperature of 105°C to remove as much as possible the moisture present in the particles. Further activation took place in an automatic electric oven of brand Heraeus, made of stainless steel, and set at a heating rate of 6.5°C/min. Different proportions of precursor materials were calcined at temperatures varying between 400 to 700°C for 30 to 120 minutes in an oven. Pure phosphoric acid from Fisher Scientific and pure sulfuric acid from JHD were used in the present work. With respect to the activating agent, the activated carbons obtained were named using the activating agents as follows: NSPT for that activated with H₃PO₄, and NSST for that activated with H₂SO₄.

2.3 Experimental design

The response surface methodology, applying central composite design was used to study the variables for preparing the activated carbons. The central composite design reduced the number of error attempts needed to evaluate the effect of interactions between the different factors that governed the process [16]. In this work, the variables whose effects were simultaneously observed are the concentration of the oxidizing agent (x_1) varying between 1 and 3 M, the calcination temperature (x_2), between 400 and 700°C and the calcination time in the oven (x_3), between 30 and 120 minutes. In practice, the total number of tests (N) performed for a composite design consists of a test number of the

factorial plane (2^k), a test number of the star plane ($2k$) and a centre test number (n_c usually ≥ 2) which is used to determine experimental errors and to verify the reproducibility of the results; and k is the number of variant factors. Hence, the number of test performed was determined from equation (1) [17],

$$N = 2^k + 2k + n_c = 2^3 + 2(3) + 3 = 17 \quad (1)$$

These experiments were done in a random way to minimize the effects of uncontrolled factors using the STATGRAPHICS Plus version 5.0 software. The expected response for each experiment was used to develop an empirical model. This model correlated the response to the three varied factors by a second-order polynomial given by equation (2) as follows [18]:

$$Y = b_0 + \sum_{i=1}^n b_i x_i + \sum_{i=1}^n b_{ii} x_i^2 + \sum_{i=1}^n \sum_{j>1}^n b_{ij} x_i x_j \quad (2)$$

where Y is the predicted response, b_0 is the constant coefficient, b_i are the coefficients of the linear terms, b_{ij} are the coefficients of the interaction terms, b_{ii} are the coefficients of the quadratic terms, while x_i and x_j are the coded values of factors that have been varied during the preparation of the activated carbons.

The expected response was the amount of iodine (IN) adsorbed (mg/g); obtained from equation (4) while the percentage yield in carbon obtained at optimal conditions was calculated using equation (3).

$$yield (\%) = \frac{m_c}{m_p} * 100 \quad (3)$$

where m_c and m_p are respectively the mass of the activated carbon and the mass of the dried precursor.

$$IN = \frac{(C_0 - C_n \cdot \frac{V_n}{2V}) \cdot M \cdot V_{ad}}{m_{CA}} \quad (4)$$

where C_0 is the initial concentration of I_2 , C_n and V_n are respectively the concentration and the volume of $Na_2S_2O_3 \cdot 5H_2O$ used for the standardization of I_2 , V_{ad} and V are respectively the volume of I_2 used for the adsorption and the volume of I_2 used for the titration; M and m_{CA} are respectively the mass in g/mol of I_2 and the mass in grams of powdered activated carbon used.

For the sake of clarity, the response (IN) was label Y_1 and Y_2 respectively for activated carbon obtained from phosphoric acid and sulfuric acid for the purposes of statistical calculations. Each of the various factors was coded according to equation 5.

$$x_i = \frac{(X_i - X_0)}{\Delta X} \quad (5)$$

where x_i is the dimensional value of independent variable, X_i represents the actual value of an independent variable i , X_0 is the actual value of the independent variable at the centre point and ΔX is the step change of X_i corresponding to a unit variation of the dimensionless quantity. The experimental variables considered in this work are shown in table 1.

Table 1: Experimental variables.

Variables	Low value -1	Centre point 0	High value 1
Activating agent concentration (M)	1	2	3
Carbonization temperature ($^{\circ}C$)	400	550	700
Carbonization time (min)	30	75	120

2.4 Physicochemical characterizations

The knowledge of the physicochemical and structural properties of any material is necessary to contribute to the understanding of several phenomena such as adsorption, desorption and others. It is in this light that the activated carbons were subjected to several characterizations.

2.4.1 Moisture content

To have a knowledge of the amount of water contained in activated carbons, the thermal drying technique as described by the standard method of the American Society for Testing and Materials (ASTM) D2866-

94 [19] was used. To achieve this, a clean and dried crucible of known mass, made of porcelain, was used. A sample of initial mass (m_i) of 0.1 g was introduced into the crucible and the assembly heated to 115 °C for 5 hours in a Binder brand oven after which it was cooled in a desiccator and weighed again. The loss in mass (m_f) of the sample after heating was hence recorded and the moisture content (M_{cont}) was calculated using equation (6).

$$M_{cont} (\%) = (m_i - m_f) \times \frac{100}{m_i} \quad (6)$$

2.4.2 Bulk density

The bulk density (B_d) of the various activated carbons was determined using Pyrex measuring cylinder of volume V_c and known mass. The sample of interest was gradually introduced and stacked manually into the cylinder up to the graduation line. After this step, the assembly was weighed using a precision Satorius brand balance 1/1000b to obtain the exact mass of the sample (m_s). The apparent density or bulk density was then deduced from equation (7).

$$B_d = \frac{m_s}{V_c} \quad (7)$$

2.4.3 Determination of surface functions by the Boehm method

The total acidic and basic functions on the surface of activated carbons were determined by the Boehm method [20]. The determination of the acidic surface functions, such as carboxylics, phenolics and lactonics, was done by putting in a closed reactor, 0.1 g of the activated carbon and 30 mL of 0.1 M solutions of Na_2CO_3 , NaHCO_3 and NaOH respectively. The basic surface functions were determined by replacing the previous basic solutions with a 0.1 M solution of HCl . The mixture was stirred by means of an Edmund Bühler GmbH multi-station stirrer at 175 rpm for 24 hours at 27°C. After filtering using a Whatman N° 4 filter paper, the filtrate was recovered. The excess basic functions contained in the filtrates, Na_2CO_3 , NaHCO_3 or NaOH was determined using the previously prepared HCl solution, while the excess acid function, HCl in the filtrates was determined using the previously prepared NaOH solution.

2.4.4 Determination of the (pH) of activated carbons

The pH is a unitless quantity generally having a magnitude between 1 and 14. It gives information on the acidic, neutral or basic nature of a solution. The pH of each activated carbon was determined using the method described by the American Society for Testing and Materials (ASTM-D3838-80). For this purpose, 0.1 g of the activated carbon was put together with 100 mL of distilled water in a closed reactor and the whole mixture stirred at 175 rpm for 24 hours at 27°C. After filtration, the pH of the filtrate was read and considered as that of the activated carbon.

2.4.5 Determination of pH at the zero point of charge (pH_{ZPC})

The pH_{ZPC} is the pH value for which a material has an overall charge of zero. The pH_{ZPC} values of the carbons were obtained from the protocol described by Lopez-Ramon *et al* (1999) [21]. In different reactors, 0.1 g of activated carbon and 30 mL of 0.1 M NaCl solution were introduced at various pH (2-10) adjusted with 0.1 M NaOH and 0.1 M HCl solutions. After stirring for 24 hours at 27°C and 175 rpm, the filtrates were collected and the final pH measured. The pH values at the zero point charge are at the intersection of the curves, $\text{pH}_{\text{initial}} = f(\text{pH}_{\text{final}})$ and the first bisector.

2.4.6 Fourier Transform Infrared Spectrophotometry (FTIR)

Infrared spectrophotometry (IR) was used to determine the functional groups within the materials as well and the type of interactions, vibration and deformation, within them. The IR spectra of the activated carbons were recorded using a Genesis FTIR™ brand spectrophotometer (ATI Mattson) equipped with a DTGS (Deuteria Tri Glycine Sulfate) detector in transmission mode between 4000 and 400 cm^{-1} .

2.4.7 Thermogravimetric analysis (TGA/TDA)

Thermogravimetric analysis (TGA/ATD) consists of measuring the variation in mass of a sample as a function of time, for a given temperature profile. The thermal decomposition of the samples was

monitored using a TGA brand thermogravimeter, NETZSCH. Approximately 10 mg of the dried samples was weighted in a platinum pan and heated from 50 to 1500°C at a heating rate of 10 K/min under nitrogen atmosphere.

2.4.8 Powder X-ray diffraction (XRD)

This technique was used to determine the crystalline or amorphous structure of the activated carbons. For this purpose, 2 mg of each dried sample was used. The diffraction patterns were recorded using an STOE Stadi-p device (STOE & Co. GmbH, Darmstadt, Germany) with a Cu K α_1 radiation ($\lambda = 1.54056$ Å, 40 kV, 30 mA). The scanning was done between 0 and 70° using a 1K detector (DECTRIS® MYTHEN) at a speed of 5°/min.

2.4.9 BET coupled with BJH

The determination of the specific surface area of a sample was based on the so-called Brunauer-Emmett-Teller (BET) equation for nitrogen adsorption [22]. The BET specific surface area of the samples were determined by N₂ adsorption at 77.13 K using a micrometric sorptometer (Thermo Electron Corporation, Sorptomatic Advanced Data Processing). *Before N₂ adsorption, the samples were subjected to vacuum at 307.13 K.* Cumulative pore volume and area were calculated using the Barrett–Joyner–Halenda (BJH) model coupled to the BET.

2.4.10 Elemental Analysis

The elemental composition of the activated carbons was determined using a Euro Vector CHNS-O element analyser (Euro EA 3000).

3. Results and discussion

3.1 Experimental design

The values of x_1 , x_2 , x_3 , as well as the predicted and experimental values of the responses Y are represented by the experimental matrix presented in Table 2. The combined effects of the different parameters were investigated statistically. The second-order complete quadratic polynomial equations have been appropriately adapted to the data and the results are presented by the regression equations 8 and 9 obtained after analysis of variance (ANOVA). Each equation gives the quantity of I₂ adsorbed as a function of the concentration of the activating agent (x_1), the carbonization temperature (x_2) and the residence time (x_3). Y_1 represents activated carbon prepared from H₃PO₄ and Y_2 that from H₂SO₄.

$$Y_1 = 949.693 + 219.714x_1 - 1.516x_2 - 0.749x_3 + 0.866x_1^2 - 0.376x_1x_2 + 0.236x_1x_3 + 0.002x_2^2 - 0.001x_2x_3 + 0.006x_3^2 \quad (8)$$

$$Y_2 = 2050.91 + 84.377x_1 - 4.254x_2 - 5.498x_3 - 43.509x_1^2 + 0.168x_1x_2 - 0.088x_1x_3 + 0.003x_2^2 + 0.002x_2x_3 + 0.029x_3^2 \quad (9)$$

From the observations made in Table 2, it appears that the predicted data of the empirical model responses are close to those obtained experimentally.

3.1.1 Analysis of variance

To study the influence of each of the parameters investigated during the preparation of NSPT and NSST samples, the importance and adequacy of the models were justified by an analysis of variance. The results obtained are reported in table 3. In general, statistical values with low probability values (p-value) indicate that they are significant for the regression model [23]. The ANOVA of the regression model demonstrates that the factors x_1 , x_2^2 , and x_3^2 were significant for the NSST response, while x_2 et x_1x_2 were significant for the NSPT response as indicated by the higher f-ratios, and values p-values ≤ 0.05 [24]. Depending on the methodology used, a model is validated for a value of correlation coefficient $R^2 \geq 0.75$ or 75%. In the present work, this value is 88.35% and 84.66% for NSST and NSPT respectively indicating a good correlation between the various factors investigated and the experimental data, which confirm the predictions.

Table 2: Experimental design matrix for optimization using CCD

H ₃ PO ₄		ACs preparation parameters		IN (mg/g), Y ₁	
Run order	H ₃ PO ₄ Concentration (x ₁)	Carbonization temperature (x ₂)	Carbonization time (x ₃)	Exp. value	Pre. value
1	2(0)	400(-1)	75(0)	701.03	728.14
2	1(-1)	550(0)	75(0)	615.61	578.22
3	1(-1)	400(-1)	30(-1)	647.45	646.55
4	3(1)	700(1)	30(-1)	562.54	561.46
5	3(1)	700(1)	120(1)	570.50	560.50
6	1(-1)	700(1)	120(1)	591.73	583.83
7	1(-1)	700(1)	30(-1)	589.08	627.25
8	2(0)	550(0)	75(0)	671.34	611.47
9	3(1)	400(-1)	120(1)	888.92	848.77
10	2(0)	550(0)	75(0)	615.81	611.47
11	2(0)	550(0)	75(0)	563.09	611.47
12	2(0)	550(0)	30(-1)	677.47	662.44
13	3(1)	400(-1)	30(-1)	809.32	815.24
14	2(0)	550(0)	120(1)	562.54	621.49
15	3(1)	550(0)	75(0)	601.13	646.44
16	2(0)	700(1)	75(0)	589.08	569.89
17	1(-1)	400(-1)	120(1)	647.45	646.55
H ₂ SO ₄		ACs preparation parameters		IN (mg/g), Y ₂	
Run order	H ₂ SO ₄	Carbonization	Carbonization	Exp.	Pre.
1	2(0)	400(-1)	75(0)	720.87	663.78
2	1(-1)	550(0)	75(0)	620.04	596.22
3	1(-1)	400(-1)	30(-1)	838.51	830.51
4	3(1)	700(1)	30(-1)	689.72	686.27
5	3(1)	700(1)	120(1)	671.34	676.84
6	1(-1)	700(1)	120(1)	644.80	642.21
7	1(-1)	700(1)	30(-1)	602.38	635.83
8	2(0)	550(0)	75(0)	666.75	635.82
9	3(1)	400(-1)	120(1)	753.59	717.64
10	2(0)	550(0)	75(0)	647.70	635.82
11	2(0)	550(0)	75(0)	612.98	635.82
12	2(0)	550(0)	30(-1)	729.71	707.63
13	3(1)	400(-1)	30(-1)	780.13	780.22
14	2(0)	550(0)	120(1)	647.45	679.53
15	3(1)	550(0)	75(0)	554.58	588.39
16	2(0)	700(1)	75(0)	678.95	646.04
17	1(-1)	400(-1)	120(1)	782.78	783.74

Exp value = experimental value; Pre value = predicted value

Table 3. Analysis of variance of Y for the activated carbons

H ₂ SO ₄ (NSST)				
Source	Df	Y ₁		
		Mean square	f-ratio	p-value
x ₁	1	153.272	0.10	0.7563
x ₂	1	34655.600	23.56	0.0018 *
x ₃	1	1973.740	1.34	0.2847
x ₁ ²	1	5071.990	3.45	0.1057
x ₁ x ₂	1	5072.7600	3.45	0.1057
x ₁ x ₃	1	124.899	0.08	0.7792
x ₂ ²	1	12789.240	8.70	0.0214 *
x ₂ x ₃	1	1412.73	0.96	0.3597
x ₃ ²	1	8938.740	6.08	0.0431 *
R ² = 88.35%				
H ₃ PO ₄ (NSPT)				
Source	Df	Y ₂		
		Mean square	f-ratio	p-value
x ₁	1	11634.200	4.09	0.0828
x ₂	1	26606.100	22.01	0.0022 *
x ₃	1	61.1078	0.02	0.8876
x ₁ ²	1	2.010	0.00	0.9795
x ₁ x ₂	1	2543.500	8.94	0.0202 *
x ₁ x ₃	1	901.214	0.32	0.5911
x ₂ ²	1	3777.970	1.33	0.2870
x ₂ x ₃	1	594.953	0.21	0.6613
x ₃ ²	1	418.708	0.15	0.7126
R ² = 84.66%				

*Significant factors; Df = degree of freedom; ACs = activated carbons

3.1.2 Response surface, Pareto diagram and main effects of factors on iodine number

The response surfaces, the Pareto diagrams and the influence of the various parameters during the preparation of the samples have been materialized in [figure 2](#).

From this figure, it is possible to establish a link in the interactions between the parameters taken into account during the production of the activated carbons. It is thus possible to observe for each of the samples the variation of the iodine number due to the synergistic effect of the factors investigated. As observed on the three dimension response surfaces ([figure 1a and 1b](#)), the iodine number decreases with increasing temperature. The same phenomenon is observed when the calcination time of the precursor increases. These observations were made when the concentration of the activating agent was kept fixed. From the observation of the different standard effects obtained through the Pareto diagrams, it appears that the temperature has a more remarkable effect compared to the interaction of the different factors involved.

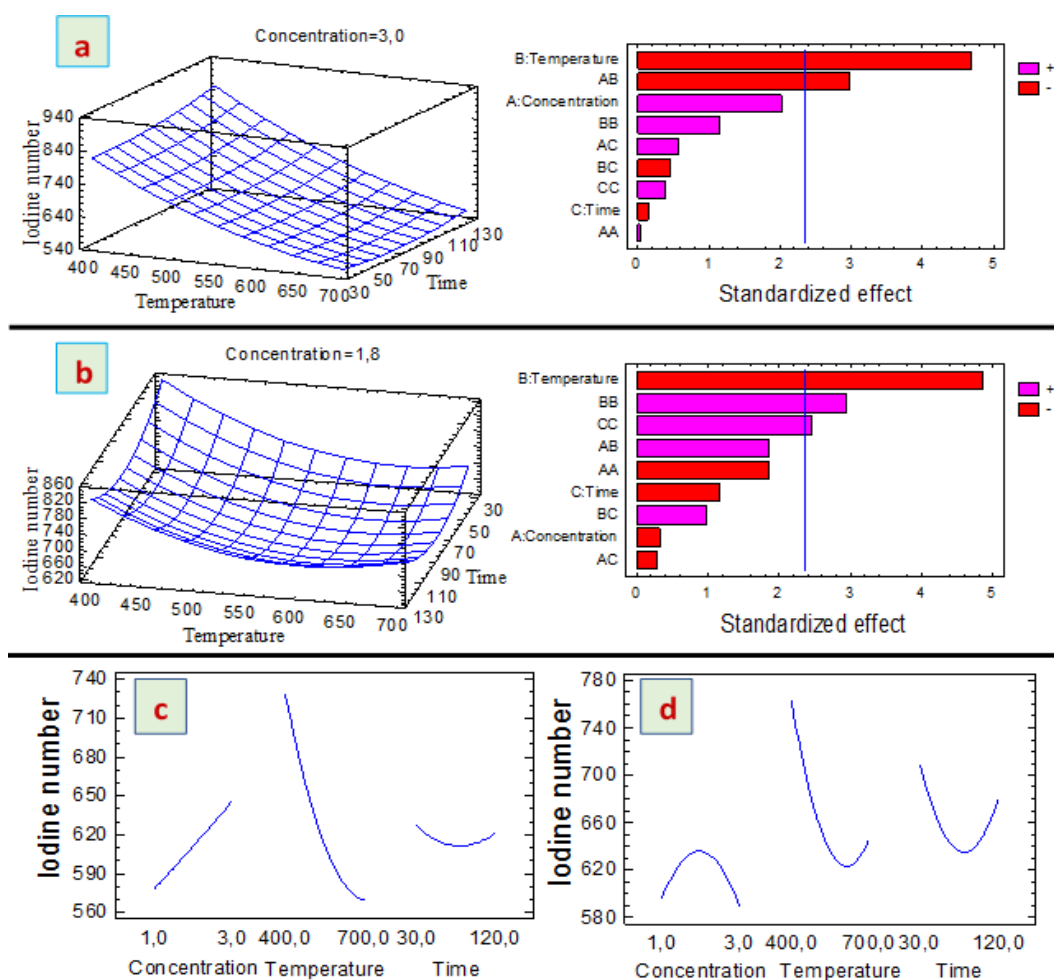


Figure 2: Three-dimensional response surfaces, Pareto diagrams: NSPT (a); NSST (b) and Effects of factors investigated: NSST (c); NSPT (d)

3.1.3 Validation of the experimental model

After obtaining the influence of the various parameters investigated, the optimal conditions predicted by the STATGRAPHICS Plus version 5.0 software were generated. When the oxidizing agent was phosphoric acid, that is, for the NSPT sample, the optimal conditions were as follows: the concentration was 3 M for a calcination time of 120 min. With regard to sulfuric acid as oxidizing agent; thus the NSST sample, these conditions were: the concentration was 1.8 M for a calcination time of 30 min. For these two samples, the calcination temperature was 400 °C. As for the iodine number, the optimal values were 848.771 mg/g and 852.506 mg/g for the NSPT and NSST ACs respectively. Results obtained experimentally from these predicted values are summarized in table 4. Yields of powdered ACs were then calculated at these optimal conditions using equation (3). The yields obtained were 53.41% and 38.85% respectively for NSPT and NSST. These relatively poor yields could be explained by the high content of fatty acid contained in the precursor. In fact, it has been reported that the fatty acid content of safou nuclei is significant: palmitic acid, 38.56%; oleic acid, 32.62%; linoleic acid, 27.30%; stearic acid, 2.18%; and linolenic acid, 1.25%) [1].

Table 4: Validation of the experimental model

	X ₁ (mol/L)	X ₂ (°C)	X ₃ (min)	Y (mg/g)		Error (%)
				Obs. value	Fit. value	
NSST	1.8	400	30	822.585	852.506	3.64
NSPT	3	400	120	838.506	848.771	1.22

Obs value = experimental value ; Fit value = predicted value

3.2. Moisture content, bulk density, pH and pH_{pzc} of activated carbons

Some of the results obtained after characterization of the NSPT and NSST ACs are listed in Table 5. From the observation of the data in this table, the values in moisture content of the carbons are 4 and 3% for the NSPT and NSST respectively. These values are good because they are in the normal range of 1 to 5%. Studies have shown that ACs with a moisture content of less than 5% allows higher adsorption of pollutants [25]. As for the apparent densities, the values are respectively 0.775 and 0.794 g/cm^3 for NSPT and NSST. These values are greater than 0.25 g/cm^3 , a value set by the American Water Work Association as the limit for a good activated carbon for practical purposes [26]. The values of the pH of NSPT and NSST are respectively 3.36 and 7.66. These materials have an acidic and basic character respectively. From figure 3, the pH at zero point charge was found to be pH_{pzc} 4.36 for NSPT and 6.94 for NSST. These results imply that in solutions with lower pH values, where $pH < pH_{pzc}$, the materials will be negatively charged and for $pH > pH_{pzc}$, they will be positively charged [27].

Tableau 5: Physicochemical characterization of NSPT and NSST carbons

ACs	M_{cont} (%)	B_d (g/cm^3)	pH	pH_{pzc}
NSPT	4	0.775	3.36	4.36
NSST	3	0.794	7.66	6.94

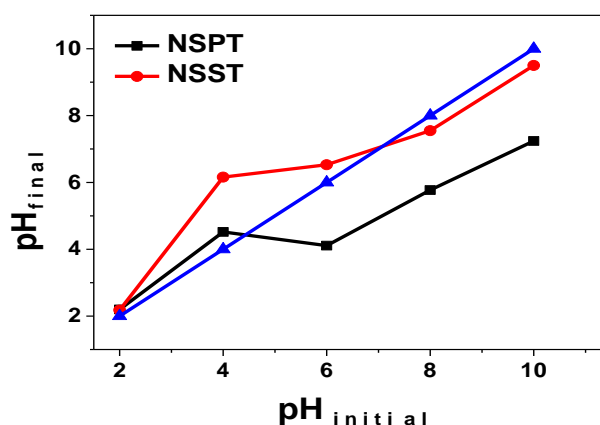


Figure 3: Determination of pH at point of zero charge (pH_{pzc})

3.3 Chemical functions of activated carbons

Quantification of the acidic and basic chemical functions of the activated carbons was done by Boehm's method. The results obtained are shown in table 6. It appears that the materials NSST and NSPT have a total acidity much higher than the total basicity. Therefore the prepared activated carbons have a dominant acid character. This result can be explained by the acid treatment applied to the precursor material on the one hand, and by the presence of fatty acids in its composition on the other hand.

Table 6: Chemical functions on the surface of the Acs

CA	Chemical Functions			Total acidity (meq/g)	Total basicity (meq/g)
	Carboxylic (meq/g)	Lactone (meq/g)	Phenolic (meq/g)		
NSST	2.86	0.32	0.36	3.63	1.95
NSPT	2.89	0.63	0.04	3.56	1.88

3.4 Elemental analysis

The elemental composition of the samples is shown in table 7 in which it can be observed that carbon which amount 76.44 for NSST and 73.503 for NSPT are greater than the other elements combined, and this is good for activating carbons.

Table 7: Elemental analysis of the activated carbons.

Sample	Elemental composition (%)				
	N	C	H	S	O ^a
NSST	2.138	76.544	3.818	0.815	16.685
NSPT	1.805	73.503	3.782	nd ^b	20.91

^a = calculated ; ^b = not detected

3.5 FTIR analysis of activated carbons

Infrared spectroscopy was used to determine the different functional groups present on the surface of the activated carbons NSPT and NSST. To better appreciate the effect of carbonization, the FTIR spectra of the raw material and the carbonized material were superimposed (figure 4).

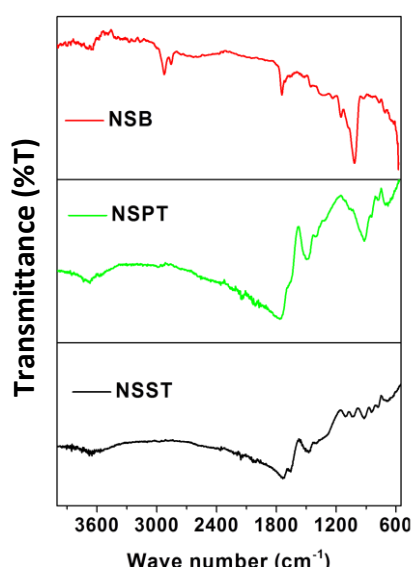


Figure 4: Superimposed IR spectra of NSB, NSPT and NSST.

The spectral pattern of the precursor (NSB) reveals at 3649.44 cm^{-1} a stretching vibration band characteristic of polysaccharides, lignin, alcohols or phenols. At 2923.87 cm^{-1} and 2854.07 cm^{-1} characteristic peaks of stretching vibrations of C-H aliphatic and CH_2 bonds was observed. A characteristic peak of C = O elongation vibrations associated with carboxylic acids and carbonyl groups (saturated and unsaturated fatty acids) was observed at 1869.73 cm^{-1} . At 1749.65 cm^{-1} , there was the characteristic peak of the deformation vibrations of C = C bonds of aromatic rings. Stretching vibrations of O = C-O in saturated and unsaturated fatty acids was observed between 1500 and 1300 cm^{-1} regions [15]. There was also a characteristic peak of elongation vibrations assigned to C-O bonding of lignin carbonyl groups between 1300 and 1200 cm^{-1} . Finally, around 900 cm^{-1} , a peak was observed which could be attributed to the elongation vibrations of the C-O-C bond of epoxides [28]. For the two activated carbons, no peaks were observed between 3649.44 cm^{-1} and 1749.65 cm^{-1} , showing that during activation and pyrolysis of the precursor material, there was decomposition of surface chemical functional groups present as oxygenated hydrocarbons, which reflect the carbohydrate structure of cellulose and hemicellulose [29]. This is due to the fact that the activation process led to the breakage of many bonds in the saturated and unsaturated fatty acid, polysaccharides, aromatic species and the elimination of volatile and light substances.

3.6 DRX analysis of powdered carbons

The diffraction patterns of NSST and NSPT are shown in figure 5. As can be seen from the figure 5, the diffraction patterns do not show any peaks that reflect a certain crystallinity of the samples. This observation confirms the amorphous nature of the activated carbons, which is an advantage for the

adsorption of chemicals, and in addition, it indicates the porous nature of the samples [30]. Moreover, the observed amorphous character confirms that NSPT and NSST may have high micro porosity [31]. Therefore, the NSB material is a good precursor for the preparation of powder activated carbons.

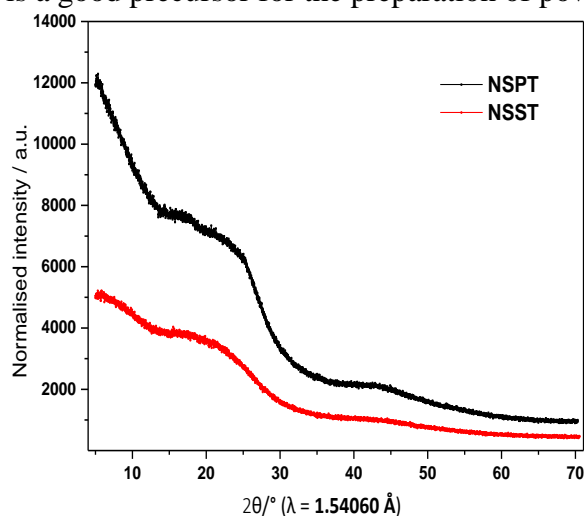


Figure 5: Powdered X-ray diffraction of NSPT and NSST samples.

3.7 Thermogravimetric analysis (TGA/TDA)

The thermal decomposition of NSST and NSPT samples, according to whether the process is endothermic or exothermic was investigated and the results are shown in figure 6.

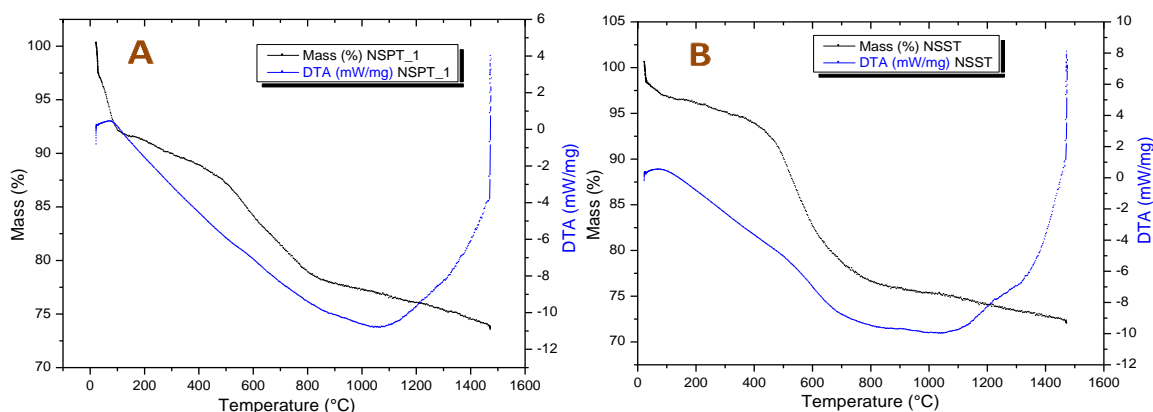


Figure 6: Pyrolysis curve (TGA/TDA): (A) = NSPT and (B) = NSST.

The TGA/TDA profiles show that the thermal process has two steps for both activated carbons. For NSPT, the large progressive loss of mass of about 34% between 100 and 200°C could be assigned to the evaporation of adsorbed water, coupled with the volatilization of hydrocarbons following an exothermic process. The second mass loss of about 46% occurred between 400 and 1200°C following an endothermic process. This loss of mass can be likened to the breaking of the weakest bonds present in the structure of the material leading to the early development of a cross-linked rigid product (graphitic layers) [32]. With regard to NSST, there is a gentle loss of mass of about 14% due to the evaporation of adsorbed water and it took place between 50-300°C following an exothermic process. This was followed by a progressive loss of a significant mass of about 60% between 310 and 1100°C due to the decomposition of organic matter resulting from an endothermic process [33]. This phenomenon was attributed to an auto-catalytic reaction which could have caused shrinkage and progressive melting of the precursor. For both samples, the second loss in mass observed corresponds to the progressive decomposition of cellulose, hemicellulose and pectin [34].

3.8 BET/BJH analysis

Nitrogen, (N_2) adsorption-desorption isotherms were investigated and the results are shown in figure. 7.

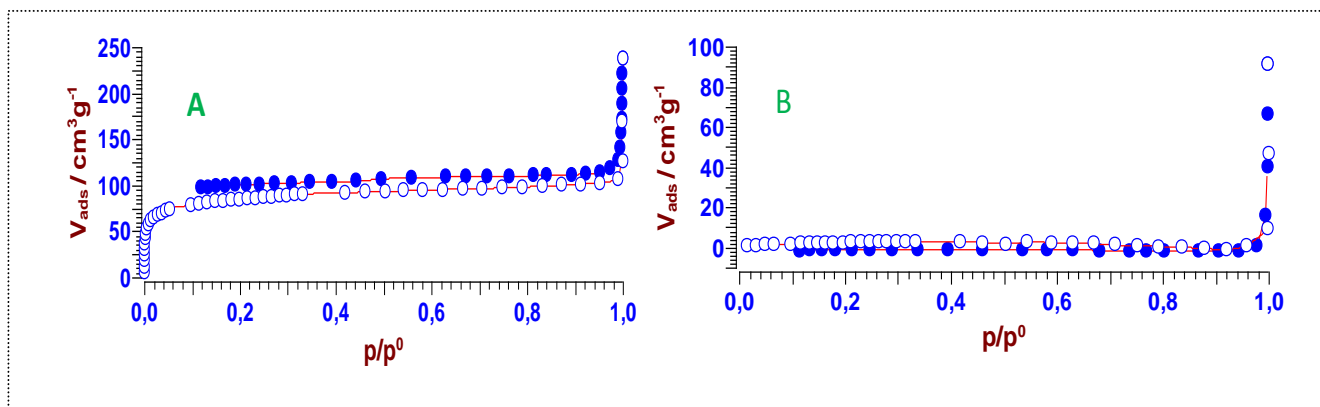


Figure 7: Adsorption curves (white background) - desorption (blue background) of nitrogen at 77.13 K: A = NSPT and B = NSST.

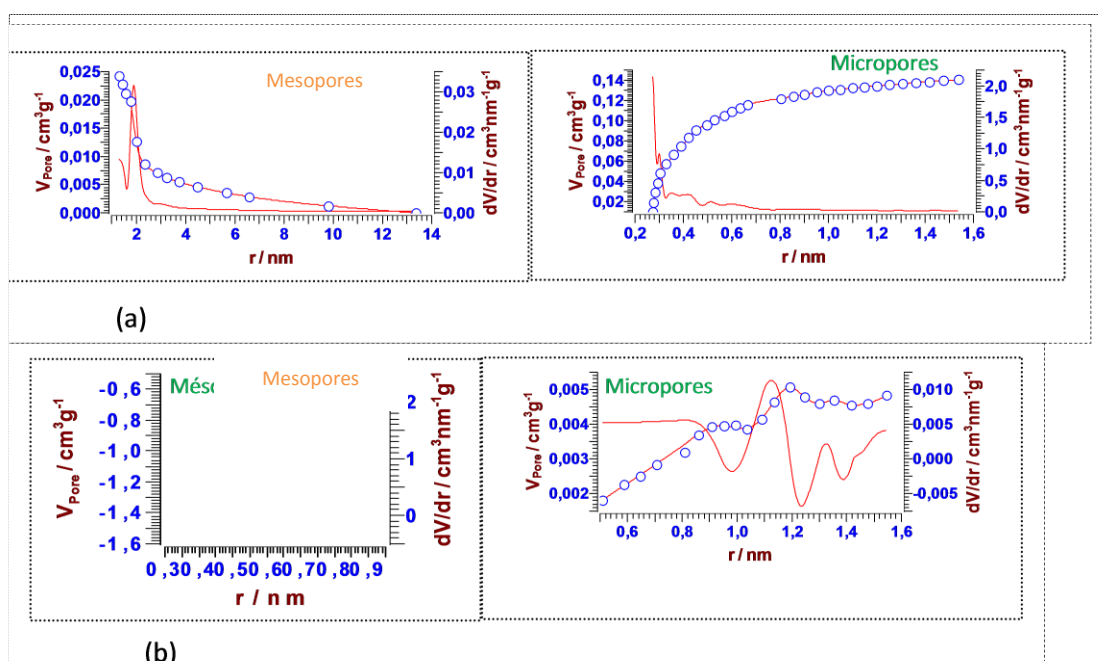


Figure 8: Sample Pore Size Distribution: (a) = NSPT and (b) = NSST

From figure 8, the mass area of each of the activated carbons NSPT and NSST was determined using the BET multipoint method at the relative pressure P/P_0 range between 0.05 and 1. From figure 7A (NSPT), the isotherm is a mixture of type I (for low values of P/P_0) and type IV (for intermediate and high values of P/P_0) according to IUPAC classification. Still from figure 7A, significant adsorption was observed from about $P/P_0 = 0.4$ with an H_4 type hysteresis loop; reflecting the simultaneous presence of micropores and mesopores [33]. In addition, a sharp increase in the adsorbed volume of N_2 was observed for values of P/P_0 greater than 0.4. This significant increase is generally associated with capillary condensation, indicating a good homogeneity of the sample [22]. A closer look at figure 7B (NSST) shows that the adsorption-desorption isotherm of N_2 is of type I. This is usually done at very low values of P/P_0 (0 and 0.35 as it is the case in this study) and is essentially specific to microporous materials according to the IUPAC classification [35]. This observation was confirmed with regard to the distribution of micropores presented in figure 8 (b) above, where there was no recorded signal for mesopores. This distribution was observed during desorption and by the Barrett, Joyner and Halenda (BJH) method. The parameters of the porous structure of the different samples were calculated and the results recorded in table 8.

Table 8: Parameters of the porous structure of NSPT and NSST

	S_{BET} (m ² /g)	Micropores			Mesopores		
		S_{BET} (m ² /g)	Cumulative pore volume (cm ³ /g)	Average pore diameter (nm)	S_{BET} (m ² /g)	Cumulative pore volume (cm ³ /g)	Average pore diameter (nm)
NSPT	326.68	443.95	0.1406	0.3745	21.249	0.0243	2.026
NSST	10.894	13.85	0.0048	1.1256		/	

Conclusion

This work was aimed at preparing two activated carbons based on safou seeds by chemical activation. Objectively, this was done by optimizing three factors that can greatly influence their properties. For the activated carbon NSPT, the optimum conditions were H₃PO₄ at 3 M, concentration, calcination time of 120 minutes, calcination temperature of 400°C. For NSST using H₂SO₄ the optimal conditions were 1.8 M, 30 minutes, 400 °C. A mathematical model based on the response surface methodology was used for this purpose. STATGRAPHICS Plus version 5.0 software was used and the factors investigated were the concentration of the activating agent, the precursor calcination temperature and the residence time in the oven. The expected response was the iodine number, and each time, the experimental values were observed to be close to the predicted values obtained. On the basis of the experimental model, the study of the influence of the above mentioned factors led to optimal conditions. Under these conditions, the response was obtained experimentally for each of the samples with an error range much less than 5% of that predicted. The pH of less than 7, as well as the dominant acid functions on the surface of the materials, shows the predominant acidic character of the synthesized activated carbons. The use of H₂SO₄ as activating agent led to the development of micropores only, while H₃PO₄ promoted the development of micropores and mesopores.

References

1. J. O. E. Otaigbe, O. G. Oriji, G. E. Ekerenam, Studies on the paint forming properties of avocado (*Persea americana*) and African pear (*Dacryodes Edulis*) seeds oils. *Int. Journal of Engineering Research and Application*, 6 (2016) 8-15. [ISSN: 2248-9622](https://doi.org/10.22207/ijera.20160608).
2. T. F. R. Tiegam; I. Ioana, N. Adina, S. G. Anagho, Optimization of the activated carbon synthesis of peanut shells, applying surface methodology. *27th European Biomass and Exhibition*, 27-30 May (2019), 1849-1855, Lisbon, Portugal. [https://doi: 10.5071/27thEUBCE2019-5EV.3.29](https://doi.org/10.5071/27thEUBCE2019-5EV.3.29).
3. S.M. Kharrazi, N. Mirghaffari, M.M. Dastgerdi, M. Soleimani. Anovel post-modification of powdered activated carbon prepared from lignocellulosic waste through thermal tension treatment to enhance the porosity and heavy metals adsorption, *Powder Technology*(2020), <https://doi.org/10.1016/j.powtec.2020.01.065>
4. Y. Guo, D.A. Rockstraw, Physicochemical properties of carbons prepared from pecan shell by phosphoric acid activation. *Bioresour. Technol*, 98 (2007) 1513–1521. <https://doi:10.1016/j.biortech.2006.06.027>.
5. A.H. Basta, V. Fierro, H. El-Saied and A. Celzard, Effect of deashing rice straws on their derived activated carbons produced by phosphoric acid activation. *Biomass and Bioenergy*, 35 (2011). <https://doi:10.1016/j.biombioE.2011.01.043>.
6. I. Tchakala.; L. Bawa Moctar, G. Djaneye Boundjou, K.S. Doni, and P. Nambo, Optimisation du procédé de preparation des charbons actifs par voie chimique (H₃PO₄) à partir des tourteaux de karité et des tourteaux de coton. *Int. J. Biol. Chem. Sci*, 6 (2012) 461-478. <https://dx.doi.org/10.4314/ijbcs.v6i1.42>.
7. V. Fierro, G. Muniz, A.H. Basta, H. El-Saied, and A. Celzard, Rice straw as precursor of activated carbons: activation by orthophosphoric acid. *J. Hazard. Mater*, 181 (2010) 27-34. <https://doi:10.1016/j.jhazmat.2010.04.062>. Epub 2020 Apr 21

8. A.H. Basta, V. Fierro, H. El-Saied, and A. Celzard, 2-Steps KOH activation of rice straw: an efficient method for preparing high-performance activated carbons. *Bioresour. Technol*, 100, (2009) 3941-3947. <https://doi:10.1016/j.biortech.2009.02.028>. Epub 2009 Apr 8.
9. L. Qingling, L. Yucheng, C. Mingyan, M. Lili, Y. Bing, L. Lingli, L. Qian. Optimized preparation of activated carbon from coconut shell and municipal sludge. *Materials Chemistry and Physics*. 241 (2020). <https://doi.org/10.1016/j.matchemphys.2019.122327>
10. F. Ghorbani, S. Kamari, S. Zamani, S. Akbari, M. Salehi. Optimization and modeling of aqueous Cr(VI) adsorption onto activated carbon prepared from sugar beet bagasse agricultural waste by application of response surface methodology, *Surfaces and Interfaces* (2020), doi: <https://doi.org/10.1016/j.surfin.2020.100444>
11. B. Karagozoglu, M. Tasdemir, E. Demirbas, M. Kobya, The adsorption of basic dye (Astrazon Blue FGRL) from aqueous solutions onto sepiolite, fly ash and apricot shell activated carbon: kinetic and equilibrium studies. *J. Hazard. Mater*, 147 (2007) 297–306. <https://doi:10.1016/j.jhazmat.2007.01.003>.
12. K.T. Idris-Hermann, T.D.R. Tchuiwon, G. Doungmo, S.G. Anagho, Preparation and characterization of activated carbons from bitter kola (*Garcinia kola*) nut shells by chemical activation method using H₃PO₄, KOH and ZnCl₂. *Chem. Sci. Int. J*, 23 (2018) 1-15. <https://doi:10.9734/CSJI/2018/43411>.
13. J.N. Sahu, S. Agarwal, B.C. Meikap, and M.N. Biswas, Performance of a modified multi-stage bubble column reactor for lead(II) and biological oxygen demand removal from wastewater using activated rice husk. *J. Hazard. Mater*, 161 (2009) 317–324. doi:10.1016/j.jhazmat.2008.03.094.
14. L. Temple, Les marchés des fruits et légumes au Cameroun. *Bulletin Équinoxe de la Coopération au Cameroun* (1999).
15. T. Kamgaing, Y.C. Sonwa, N.J.J. Kouonang, G. Doungmo, M.M.F. Tchieno, and M.J. Ketcha, Safou (*Dacryodes Edulis*) seeds applied to the removal of bisphenol A in solution. Implication of surface antioxidant molecules on the chemical sorption of the endocrine disruptor. *Int. J. Curr. Res*, 9 (2017) 49792-49801. [ISSN: 0975-833X](https://doi.org/10.1016/j.ijcr.2017.09.031).
16. I. A.W. Tan, A.L. Ahmad, B.H. Hameed, Optimization of preparation conditions for activated carbons from coconut husk using response surface methodology. *Chem. Eng J*, 137 (2008) 462–470. <https://doi:10.1016/j.cej.2007.04.031>.
17. M.S. Tanyildizi, Modeling of adsorption isotherms and kinetics of reactive dye from aqueous solution by peanut hull. *Chem. Eng. J*, 168, (2011) 1234–1240. doi:10.1016/j.cej.2011.02.021.
18. G.E.B. Box, W.G. Hunter, and J.S. Hunter, *Statistics of experimenters, and introduction to design, data analysis, model building*. Wiley Edition, New York, (1978) 653p. [ISBN 0471093152, 9780471093152](https://doi.org/10.1002/9780471093152).
19. O.A. Ekpete, M.J. Horsfall, Preparation and characterization of activated carbon derived from fluted pumpkin stem waste (*telfairiaoccidentalis* Hook F). *Res. J. Chem. Sci*, 1 (2011) 10-17.
20. H. Boehm, E. Diehl, W. Heck, and R. Sappok, Surface oxides of carbon. *Angew. Chem. Internat. Edit*, 3 (1964) 1-9. <https://doi.org/10.1002/anie.196406691>.
21. M.V. Lopez-Ramon, C. Moreno-Castilla. and F. Carrasco-Marin. On the characterization of acidic and basic surface sites on carbons by various techniques. *Carbon*, 37 (1999) 1215-1221. [https://doi:10.1016/S0008-6223\(98\)00317-0](https://doi:10.1016/S0008-6223(98)00317-0).
22. T. Sreethawong, S. Chavadej, S. Ngamsinlapasathian, S and S. Yoshikawa, A modified sol-gel process-derived highly nanocrystalline mesoporous NiO with narrow pore size distribution. *Colloids. Surf. A. Physicochem. Eng. Asp*, 296 (2007) 222–229. doi:10.1016/j.colsurfa.2006.09.048.
23. S. Sugashini and K.M.S. Begum, Optimization using central composite design (CCD) for the biosorption of Cr(VI) ions by cross linked chitosan carbonized rice husk (CCACR). *Clean Technol Envir*, 15 (2013) 293-302. <https://doi:10.1007/s10098-012-0512-3>.
24. J.N. Sahu, J. Acharya, and B.C. Meikap, Optimization of production conditions for activated carbons from Tamarind wood by zinc chloride using response surface methodology, *Bioresour Technol*, 10 (2010) 1974–1982. <https://doi:10.1016/j.biortech.2009.10.031>. Epub 2009 Nov 12.

25. H.G. Rhoda, O. Ideyonbe, Production of activated carbon and characterization from Snail Shell Waste (*Helix pomatia*). *Adv. Chem. Engineer. Sci*, 5 (2015) 51-61. [dx.doi.org/10.4236/aces.2015.51006](https://doi.org/10.4236/aces.2015.51006).
26. T.D.R. Tchuifon, S.G. Anagho, G.N. Nche, J.M. and Ketcha, Adsorption of salicylic and sulfosalicylic acid onto powdered activated carbon prepared from rice and coffee husks. *Int. J. Curr. Eng. Technol*, 5 (2015) 1641-1652. E-ISSN 2277-4106, P-ISSN 2347-5161.
27. N.J. Ndi, J.M Ketcha, G.S Anagho, N.J. Goghomu, E.P. Belibi, Physical and chemical characteristics of activated carbon prepared by pyrolysis of chemically treated cola nut (*cola acuminata*) shells wastes and its ability to adsorb organics, *Int. J. Adv. Chem. Technol*, 3 (2014) 1-13.
28. J.V. Nabais, P. Carrot, M.M.L. Ribeiro Carrot, V. Luz, A.L. Ortiz, Influence of preparation conditions in the textural and chemical properties of activated carbons from a novel biomass precursor: the coffee endocarp. *Bioresour. Technol*, 99 (2008) 7224-7231. <https://doi.org/10.1016/j.biortech.2007.12.068>. Epub 2008 Feb 8.
29. N.S. Nasri, H. Basri, A. Garba, U.D. Hamza, J. Mohammed, A.M Musa, Synthesis and characterization of low-cost porous carbon from palm oil shell waste via K_2CO_3 chemical activation process. *Appl. Mech. Mater*, 173 (2015) 36-40. [doi:10.4028/www.scientific.net/AMM.735.36](https://doi.org/10.4028/www.scientific.net/AMM.735.36).
30. W. Tongpoothorn, M. Sriuttha, P. Homchan, S. Chanthai, and C. Ruangviriyachai, Preparation of activated carbon derived from jatropha curcas fruit shell by simple thermochemical activation and characterization of their physicochemical properties. *Chem. Eng. Res. Des*, 89 (2011) 335-340. [doi:10.1016/j.cherd.2010.06.012](https://doi.org/10.1016/j.cherd.2010.06.012).
31. J. Zhao, L. Yang, F. Li, R. Yu, and C. Jin, Structural evolution in the graphitization process of activated carbon by high pressure sintering. *Carbon*, 47 (2009). 744-751. [doi:10.1016/j.carbon.2008.11.006](https://doi.org/10.1016/j.carbon.2008.11.006).
32. H. Yang, R. Yan, H. Chen, D. Ho Lee, and C. Zheng, Characteristics of hemicellulose, cellulose and lignin pyrolysis. *Fuel*, 86 (2007) 1781-1788. <https://doi.org/10.1016/j.fuel.2006.12.013>.
33. Y. Sun, Q. Yue, B. Gao, L. Huang, X. Xu and Q. Li, Comparative study on characterization and adsorption properties of activated carbons with H_3PO_4 and $H_4P_2O_7$ activation employing *Cyperus alternifolius* as precursor. *Chem. Eng. J*, 181-182 (2012) 790-797. [doi:10.1016/j.cej.2011.11.098](https://doi.org/10.1016/j.cej.2011.11.098).
34. A. Kumar, L. Wang, Y.A. Dzenis, D.D. Jones, and M.A. Hana, Thermogravimetric characterization of corn stover as gasification and pyrolysis feedstock. *Biomass and Bioenergy*, 32 (2008) 460-467. <https://doi.org/10.1016/j.biombioe.2007.11.004>.
35. F. Rouquerol, J. Rouquerol and K. Sing, Adsorption by powders and porous solids. Elsevier, (1999) 467 p. <https://sci-hub.tw/https://doi.org/10.1016/B978-0-12-598920-6.X5000-3>.

(2020) ; <http://www.jmaterenvironsci.com>